Intrinsic Photoconductivity of Ultracold Fermions in Optical Lattices

J. Heinze,[1] J. S. Krauser,[1] N. Fläschner,[1] B. Hundt,[1] S. Götze,[1] A. P. Itin,[1,2,3] L. Mathey,[1,2] K. Sengstock,[1,2,*] and C. Becker[1,2]

[1]*Institut für Laser-Physik, Universität Hamburg, Luruper Chaussee 149, 22761 Hamburg, Germany*
[2]*Zentrum für Optische Quantentechnologien, Universität Hamburg, Luruper Chaussee 149, 22761 Hamburg, Germany*
[3]*Space Research Institute, Russian Academy of Sciences, 117997 Moscow, Russia*

(Received 20 August 2012; revised manuscript received 7 December 2012; published 19 February 2013)

We report on the experimental observation of an analog to a persistent alternating photocurrent in an ultracold gas of fermionic atoms in an optical lattice. The dynamics is induced and sustained by an external harmonic confinement. While particles in the excited band exhibit long-lived oscillations with a momentum-dependent frequency, a strikingly different behavior is observed for holes in the lowest band. An initial fast collapse is followed by subsequent periodic revivals. Both observations are fully explained by mapping the system onto a nonlinear pendulum.

DOI: 10.1103/PhysRevLett.110.085302 PACS numbers: 67.85.−d, 03.75.Ss, 37.10.Jk, 72.20.Jv

Photoconductivity describes the change of a material's conductivity following an excitation with photons. If the photon energy is resonant with a band transition, electrons are excited from the valence band to the conduction band and an initial insulator becomes conducting [1]. Today, photoconductivity is widely used in technological applications such as semiconductor photodiodes and photoresistors. It also provides a powerful probe for novel materials, such as graphene [2], transistors made from carbon nanotubes [3], or semiconductor nanowires [4]. To extend the understanding of such complex materials, atomic quantum gases have proven to be powerful model systems. In this context it is desirable to develop and adopt versatile probing methods [5–7]. Owing to its excitational structure in several bands, photoconductivity can provide deeper insight into intra- and interband dynamics as well as orbital effects, which gained much interest in recent years. In the field of quantum gases, multiband interactions and dynamics have been experimentally studied mainly with bosonic atoms [8–17], whereas little work has been performed with fermionic atoms [18–20].

In this Letter, we thoroughly study experimentally and theoretically the particle and hole dynamics of fermionic atoms in an optical lattice. Analogous to photoconductivity measurements in solid state physics, we create uncoupled particle and hole excitations using lattice amplitude modulation. The subsequent dynamics in the combined harmonic and periodic potential is reminiscent of a nonlinear pendulum, which is a paradigm for nonlinear dynamics and is used to model many different quantum systems, like ultracold bosons in a double-well potential [21], spinor Bose-Einstein condensates [22], semiconductor heterostructures [23], and Josephson junctions [24]. In an optical lattice, each individual band independently resembles a pendulum with a different nonlinearity, leading to very distinct dynamics. As a direct consequence, the atoms in the excited band undergo pronounced long-lived oscillations with a momentum-dependent frequency. In strong contrast, we observe a fast closing of the holes in the lowest energy band followed by periodic rephasings with a slowly decaying revival amplitude. This behavior stems from the stronger nonlinearity in the lowest energy band caused by the smaller bandwidth as compared to the excited band.

In photoconductivity measurements, insulators or semiconductors are irradiated with photons which excite electrons to the conduction band at the same time leaving vacancies in the valence band (holes). Both particle and hole excitations lead to finite conductivity, which can be measured via a photocurrent induced by an external potential. In our system, the photons are mimicked by lattice amplitude modulation, which transfers zero quasimomentum to the system. The frequency of the modulation determines the excitation energy and the initial quasimomentum q_0 [see Fig. 1(a)]. In close analogy to conventional photoconductivity, we create particle (hole) excitations in the second excited (lowest) energy band of the optical lattice, corresponding to the conduction (valence) band. Note that the created excitations are localized in momentum space in contrast to spatially localized particle-hole excitations in, e.g., Mott insulating systems. Instead of measuring a current through the system, we follow the periodic dynamics of the atoms completely momentum resolved using absorption imaging after time of flight. The specific dynamics of particle and hole excitations is induced by an external harmonic confinement, typical for ultracold atom experiments. The total Hamiltonian including harmonic and periodic potential has the form

$$H = \frac{p^2}{2m} + sE_r \cos(k_{BZ}x)^2 + \frac{1}{2}m\omega_0^2 x^2, \qquad (1)$$

with the particle mass m, $E_r = \hbar^2 k_{BZ}^2/2m$, $k_{BZ} = 2\pi/\lambda$, the lattice laser wavelength λ, and the external trapping frequency ω_0. s determines the lattice depth. The time

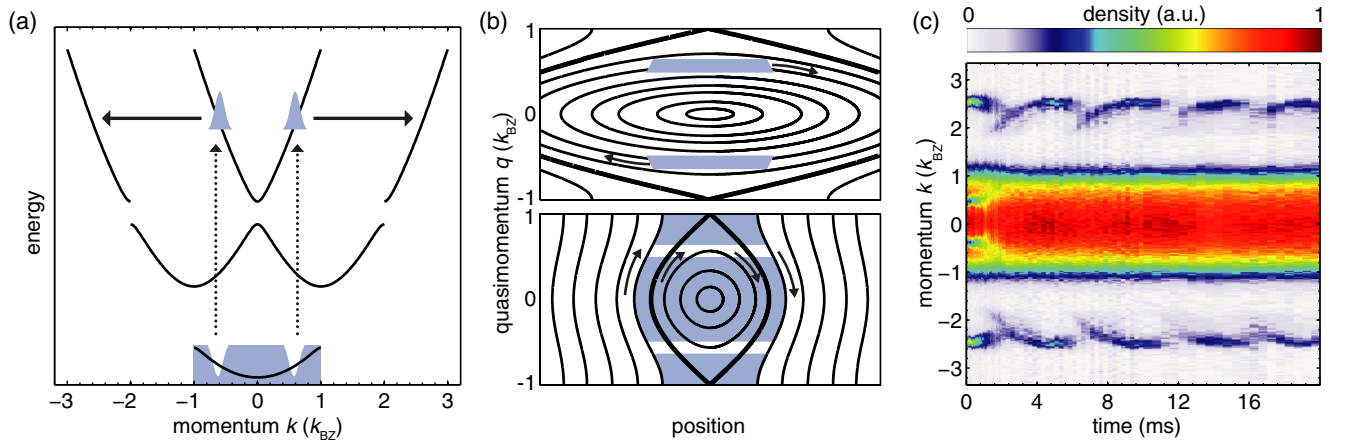

FIG. 1 (color online). (a) Principle of particle and hole excitation at a certain quasimomentum q_0 via lattice amplitude modulation (dotted lines) and subsequent band mapping process (solid lines) in momentum space. (b) Sketch of the semiclassical phase space of the lowest band (bottom) and second excited band (top). Solid lines depict equal-energy orbits. The shaded area corresponds to the occupied phase space after the lattice amplitude modulation. Due to the different bandwidths, the excited particles occupy only a small region of phase space around a single equal-energy orbit, while the holes are spread over many different orbits. The phase space evolution takes place clockwise along equal-energy orbits (indicated by arrows). (c) Typical photocurrent measurement after excitation to the excited band at $10E_r$. Shown are the column densities of the momentum distribution at different times after the excitation. Atoms in the lowest band are represented by the central plateau. The excitations in the upper band clearly oscillate in momentum space.

evolution of fermions in such a potential can be described in a semiclassical phase space [25]. In the tight-binding and single-band approximation, the corresponding energy function H_{SC} has the form of a nonlinear pendulum, with momentum and position interchanged [26],

$$H_{SC}(x, q) = -2J\cos(\pi q) + \frac{\nu}{2}x^2, \qquad (2)$$

where $\nu = m\omega_0^2(\lambda/2)^2$ and J is the tunneling matrix element [19]. If the tight-binding approximation is not valid, the momentum-dependent part $-2J\cos(\pi q)$ must be replaced by the band dispersion $E_q^{(n)}$. This leads to a nonlinear pendulum with a slightly different potential energy than in (2). Figure 1(b) shows the phase space both for the lowest band and the second excited band. Note the existence of a separatrix, where all inner states correspond to closed orbits and all outer states are localized in space [27]. For the excited band the phase space volume contained within the separatrix is much more extended along the coordinate space direction as compared to the lowest band. This is due to the different bandwidths given by the individual energy dispersions $E_q^{(n)}$ and leads to the pronounced difference in the behavior of particles in the excited band compared to holes in the lowest band discussed below.

To measure the time evolution of the photocurrent, we prepare either a spin-polarized, noninteracting Fermi gas with $m = 9/2$ or an interacting binary spin mixture of $m = -9/2$ and $m = -5/2$ in the $f = 9/2$ ground state manifold of ^{40}K [28]. We excite the system via lattice modulation [19,29,30] and detect the quasimomentum distribution by performing adiabatic band mapping followed by resonant absorption imaging after typically 15 ms time of flight [19,31]. Recall that the band mapping technique maps particles in the different bands onto their respective Brillouin zones.

A typical time evolution in a noninteracting gas is shown in Fig. 1(c). The atoms in the excited band exhibit a pronounced oscillation in momentum space. Note that the excitations carry no net current, since always two counterpropagating excitations with quasimomenta q and $-q$ are created due to the inversion symmetry of the band structure. The lifetime of the excitations is on the order of 100 ms, which indicates a recombination between particles and holes that is slow relative to the typical oscillation period. In contrast, for these specific experimental parameters, the holes in the lowest energy band apparently close very fast within the first 2 ms.

Related results have been obtained in Ref. [13], using bosonic atoms excited to higher bands. In contrast, with fermions we are able to create and to observe elementary hole excitations, as well as obtain a full momentum resolution for the dynamics in higher bands. This is due to the Pauli principle, i.e., the population of a Fermi sea, fundamentally different from a Bose-Einstein condensate consisting of only one single macroscopically occupied wave function, where the concept of a hole in momentum space is not meaningful and the momentum resolution is limited by the very small momentum width in the lowest band. Both aspects are at the heart of the results presented in the following. We first concentrate on the excited particles and later comprehensively discuss the hole dynamics. Figures 2(a) and 2(b) show the results of photocurrent measurements for a large set of different parameters.

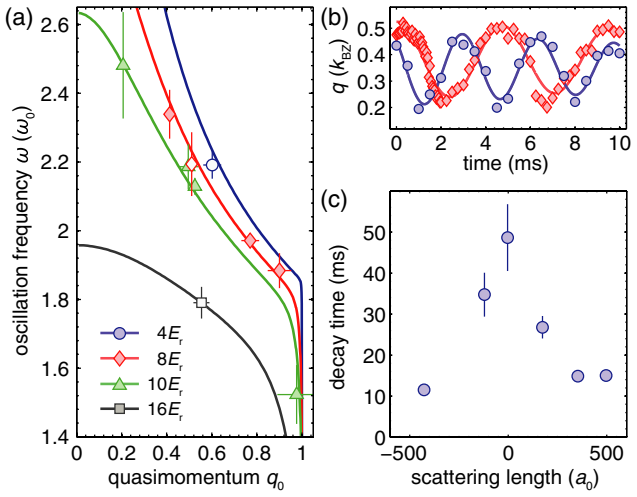

FIG. 2 (color online). (a) Comparison of measured frequencies with the results of (3) for different lattice depths and quasimomenta. Filled symbols represent measurements with noninteracting mixtures. Open symbols show data with interacting mixtures. (b) Oscillations in momentum space of the particles in the excited band at $10E_r$ for two different trapping frequencies, $\omega_0 = 2\pi \times 66$ Hz (circles) and $\omega_0 = 2\pi \times 50$ Hz (diamonds). Solid lines are fits to the data. Extracted oscillation frequencies are $\omega = 2\pi \times (148 \pm 5)$ Hz (circles) and $\omega = 2\pi \times (107 \pm 2)$ Hz (diamonds). (c) $1/e$ lifetime of particles in the second excited band as a function of the scattering length for a three-dimensional lattice of $8E_r$. All error bars solely correspond to fit errors, representing two standard deviations.

Three key observations can be drawn from the experimental data: First, the oscillation frequency ω linearly depends on the bare trapping frequency ω_0. Second, ω strongly depends on the initial quasimomentum q_0, and third, ω decreases with increasing lattice depth s.

We now explain all of these observations within the semiclassical nonlinear pendulum picture. As shown in Fig. 1(b), the excited particles are well localized in the phase space of the upper band and occupy approximately only one single equal-energy orbit. Hence, we model them as a single point in phase space with a given initial quasimomentum q_0 and corresponding energy $E(q_0)$, located at the center of the trap. With these initial conditions, the resulting equations of motion can be solved to yield [28]

$$\omega(q_0) = \omega_0 \frac{\pi}{2} \left(\int_0^{q_0} dq \sqrt{\frac{E_r}{E_{q_0}^{(2)} - E_q^{(2)}}} \right)^{-1}. \qquad (3)$$

The results of (3) are shown in Fig. 2(a) in comparison to the experimental data and show excellent agreement: Equation (3) directly confirms the linear dependence of ω on ω_0. More generally, the strong dependence of ω on q_0 is an immediate consequence of the nonlinear pendulum behavior. In particular, for $q_0 \to \pm 1$, the excitation approaches the separatrix, where the nonlinear pendulum dynamics is dramatically slowed down and the system eventually reaches a steady state. This is reflected in the strong decrease of the observed frequencies at large q_0, visible in Fig. 2(a). The dependence of ω on the lattice depth stems from the dependence of the band dispersion $E_q^{(2)}$ on s in (3). For small q_0, corresponding to small displacements of the pendulum, which lead to a harmonic oscillator behavior, this can be explained in an intuitive picture. In this case, the oscillation frequency depends on the curvature of $E_q^{(2)}$ around $q = 0$, which is $d^2E_q^{(2)}/dq^2|_{q=0}$. This curvature decreases with increasing lattice depth, leading to a corresponding decrease of ω as observed in the experiment. To check the validity of the semiclassical approach, we compared the results of (3) with a numerical single particle calculation using (1) and find perfect agreement, as shown in Ref. [28].

We further investigated the influence of interactions on the dynamics and lifetime of the particles in the excited band using a Feshbach resonance at 224 G [32]. We observe no effect on the oscillation frequency, whereas we find a substantially reduced lifetime of the atoms in the second excited band for stronger interactions as shown in Fig. 2(c). Since the total loss of particles is independent of the scattering length as we checked independently, these results can be regarded as a measure for the recombination of particles and holes.

We now return to the hole dynamics in the lowest energy band. In the photoconduction measurement of Fig. 1(c), we observe a fast reduction of the hole depth within a few ms. This is shown in detail in Fig. 3(a), for a set of different trapping frequencies. The fast closing cannot be explained by recombination with excited atoms, which have a much longer lifetime, as outlined in the preceding paragraph.

To describe the holes theoretically, we adopt a description from solid state physics, where holes in a completely filled valence band can be regarded as particles with negative mass [28]. As sketched in Fig. 4, the phase space distribution of the hole spans over many different equal-energy orbits. This crucial difference as compared to the excited atoms stems from the much smaller bandwidth of the lowest energy band and leads to more complicated dynamics for the holes. Initially, the phase space distribution basically rotates, leading to a fast reduction of the observed hole depth, which is obtained by projecting the phase space distribution onto the quasimomentum axis. For small lattice depth this rotation persists for longer times leading to a revival of the hole in quasimomentum space after multiples of half a rotation in phase space. Indeed, in a measurement specifically addressing this parameter regime, we are able to observe this coherent hole dynamics [Figs. 3(b) and 3(d)]. For strongly nonlinear systems, as realized in deeper lattices, the revival is prevented, since the nonlinearity leads to a deviation from the simple rotation by introducing momentum-dependent oscillation frequencies as in the excited band. Especially for states

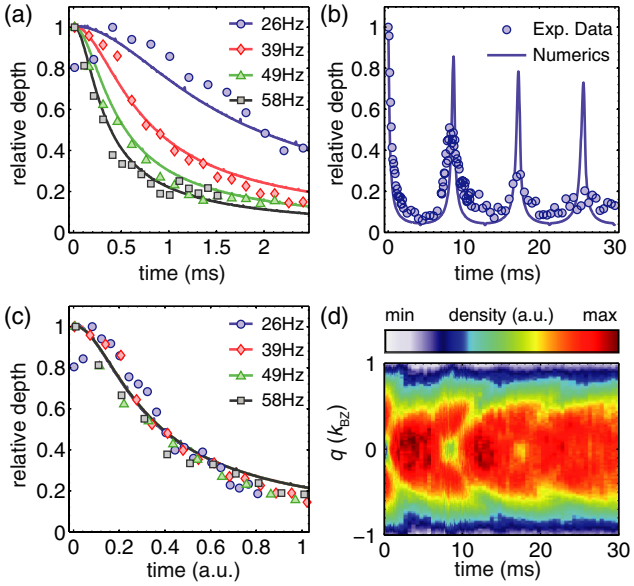

FIG. 3 (color online). (a) Time evolution of hole depth relative to the maximum depth at $10E_r$ and $q_0 = 0.5$ for different trapping frequencies $\omega/2\pi$, as given in the legend. Solid lines are semiclassical simulations as described in the text. (b) Rephasing of the hole in quasimomentum for longer evolution times at $2E_r$, $q_0 = 0.0$, and $\omega_0 = 2\pi \times 63$ Hz. Solid line is a semiclassical simulation. (c) Rescaled time evolutions from (a) with scaling factors ω_0^2 as derived from (4). The different simulations are not discernible due to the perfect scaling behavior. (d) Momentum resolved data of (b). Only the first Brillouin zone is depicted.

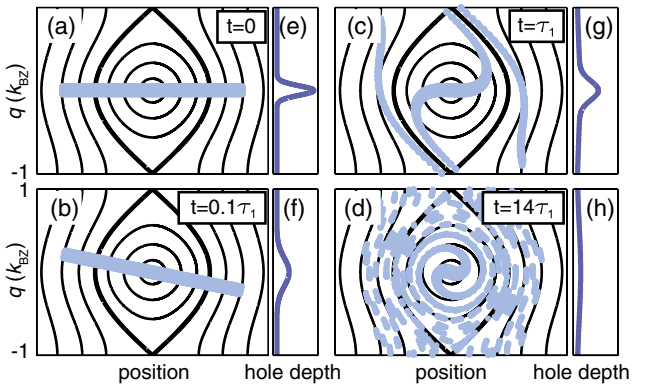

FIG. 4 (color online). (a)–(d) Sketch of the hole dynamics at $q_0 = 0$. For short times, the distribution predominantly rotates. For certain parameters a periodic revival of the hole is observed. For long times $t \gg \tau_1$ all trajectories dephase and the hole signature is lost. (e)–(f) Projection of the hole distribution onto momentum space.

outside the separatrix, this leads to a fast dephasing of the initial phase space distribution, resulting in an irreversible disappearance of the holes on our experimental time scales.

To explore the de- and rephasing of the holes in the nonlinear pendulum picture, we performed simulations on the semiclassical phase space, using the truncated Wigner approximation method [33,34] for an initial hole distribution which is Gaussian both in momentum and spatial coordinates, with a width Δq in momentum space and $\Delta x = 1/\Delta q$ in coordinate space. This corresponds to a coherent superposition of lattice eigenstates as explained in Ref. [28]. Figures 3(a) and 3(b) demonstrate the excellent agreement of the simulations with our experimental data. Within the semiclassical description, it is also possible to derive an analytical expression for the hole dynamics valid for times $t \ll \tau_1, \tau_2$. $\tau_1 = h/\sqrt{2J\nu}$ is the typical time scale for a full rotation in phase space at small amplitudes. $\tau_2 = \hbar\Delta x/\pi J \sin^2(\pi q_0)$ is the time scale for the change of the real space distribution due to the phase space rotation. We find the time-dependent depth $D(t)$ of the hole to be [28]

$$D(t) = \frac{D(t=0)}{\sqrt{1 + (t/T)^2}}. \tag{4}$$

$T = \hbar\pi^2\Delta q^2/\nu$ compares the hole width in momentum space Δq to the trap energy, which is a measure for the coupling of different momentum states. Thus T sets the time scale for changes in the momentum distribution due to rotations in phase space. From (4) we find that the holes are stabilized for broader wave packets and lower trapping frequencies. In particular, the hole depth scales as $T \propto 1/\omega_0^2$, which allows for stable holes even at moderately low trapping frequencies. Figure 3(c) shows the rescaled simulations and experimental data, confirming the $1/\omega_0^2$ scaling. As for the excited particles, we performed single particle calculations with (1) and find very good agreement with the semiclassical description for all parameters [28].

In conclusion we have presented a comprehensive study of the dynamics of an excited Fermi gas in an optical lattice, reminiscent of photoconductivity measurements in solids which extends the available techniques to explore dynamical properties of optical lattice systems. We obtain an intuitive and quantitative description of all experimental findings by mapping our system onto the semiclassical phase space of a nonlinear pendulum. In particular, this correctly describes the strikingly different dynamics of particles in the excited band and holes in the lowest energy band. Our results provide the first investigation of holes in momentum space in an ultracold quantum gas in an optical lattice and thus constitute an important contribution towards a more complete understanding of ultracold atoms in periodic potentials. They may also prove crucial for further studies on particle-hole excitations such as excitons [35] and give strong connections to exciting condensed matter systems, which show a similar dynamical behavior [23,24].

We thank P. Törmä for valuable discussions. We acknowledge financial support by DFG via Grant No. FOR801. L. M. and A. P. I. acknowledge support from DFG (Grant No. SFB 925) and the

Landesexzellenzinitiative Hamburg, which is financed by the Wissenschaftsstiftung Hamburg and supported by the Joachim Herz Stiftung. J. Heinze, J. S. Krauser, and N. Fläschner contributed equally to this work.

*Corresponding author.
klaus.sengstock@physnet.uni-hamburg.de

[1] R. H. Bube, *Photoconductivity in Solids* (Wiley, New York, 1960).
[2] E. J. H. Lee, K. Balasubramanian, R. T. Weitz, M. Burghard, and K. Kern, Nat. Nanotechnol. **3**, 486 (2008).
[3] M. Freitag, J. C. Tsang, A. Bol, D. Yuan, J. Liu, and P. Avouris, Nano Lett. **7**, 2037 (2007).
[4] Y. Ahn, J. Dunning, and J. Park, Nano Lett. **5**, 1367 (2005).
[5] D. Jaksch, C. Bruder, J. I. Cirac, C. W. Gardiner, and P. Zoller, Phys. Rev. Lett. **81**, 3108 (1998).
[6] M. Lewenstein, A. Sanpera, V. Ahufinger, B. Damski, A. Sen, and U. Sen, Adv. Phys. **56**, 243 (2007).
[7] I. Bloch, J. Dalibard, and W. Zwerger, Rev. Mod. Phys. **80**, 885 (2008).
[8] E. Peik, M. BenDahan, I. Bouchoule, Y. Castin, and C. Salomon, Phys. Rev. A **55**, 2989 (1997).
[9] T. Salger, C. Geckeler, S. Kling, and M. Weitz, Phys. Rev. Lett. **99**, 190405 (2007).
[10] T. Müller, S. Fölling, A. Widera, and I. Bloch, Phys. Rev. Lett. **99**, 200405 (2007).
[11] D. Clément, N. Fabbri, L. Fallani, C. Fort, and M. Inguscio, New J. Phys. **11**, 103030 (2009).
[12] P. T. Ernst, S. Götze, J. S. Krauser, K. Pyka, D.-S. Lühmann, D. Pfannkuche, and K. Sengstock, Nat. Phys. **6**, 56 (2010).
[13] J. F. Sherson, S. J. Park, P. L. Pedersen, N. Winter, M. Gajdacz, S. Mai, and J. Arlt, New J. Phys. **14**, 083013 (2012).
[14] T. Salger, C. Grossert, S. Kling, and M. Weitz, Phys. Rev. Lett. **107**, 240401 (2011).
[15] G. Wirth, M. Ölschläger and A. Hemmerich, Nat. Phys. **7**, 147 (2011).
[16] N. Fabbri, S. D. Huber, D. Clément, L. Fallani, C. Fort, M. Inguscio, and E. Altman, Phys. Rev. Lett. **109**, 055301 (2012).
[17] P. Soltan-Panahi, D.-S. Lühmann, J. Struck, P. Windpassinger, and K. Sengstock, Nat. Phys. **8**, 71 (2012).
[18] M. Köhl, H. Moritz, T. Stöferle, K. Günter, and T. Esslinger, Phys. Rev. Lett. **94**, 080403 (2005).
[19] J. Heinze, S. Götze, J. S. Krauser, B. Hundt, N. Fläschner, D.-S. Lühmann, C. Becker, and K. Sengstock, Phys. Rev. Lett. **107**, 135303 (2011).
[20] L. Tarruell, D. Greif, T. Uehlinger, G. Jotzu, and T. Esslinger, Nature (London) **483**, 302 (2012).
[21] A. Smerzi, S. Fantoni, S. Giovanazzi, and S. R. Shenoy, Phys. Rev. Lett. **79**, 4950 (1997).
[22] W. Zhang, D. L. Zhou, M.-S. Chang, M. S. Chapman, and L. You, Phys. Rev. A **72**, 013602 (2005).
[23] K. N. Alekseev and F. V. Kusmartsev, Phys. Lett. A **305**, 281 (2002).
[24] P. W. Anderson, *Lectures on the Many-Body Problem*, edited by E. R. Caianello (Academic, New York, 1964).
[25] L. Pezzè, L. Pitaevskii, A. Smerzi, and S. Stringari, G. Modugno, E. DeMirandes, F. Ferlaino, H. Ott, G. Roati, and M. Inguscio, Phys. Rev. Lett. **93**, 120401 (2004).
[26] A. R. Kolovsky and H. J. Korsch, Int. J. Mod. Phys. B **18**, 1235 (2004).
[27] H. Ott, E. de Mirandes, F. Ferlaino, G. Roati, V. Türck, G. Modugno, and M. Inguscio, Phys. Rev. Lett. **93**, 120407 (2004).
[28] For details see online Supplemental Material at http://link.aps.org/supplemental/10.1103/PhysRevLett.110.085302 for the atomic sample preparation, the data evaluation, and the semiclassical and numerical calculations.
[29] J. H. Denschlag, J. E. Simsarian, H. Häffner, C. McKenzie, A. Browaeys, D. Cho, K. Helmerson, S. L. Rolston, and W. D. Phillips, J. Phys. B **35**, 3095 (2002).
[30] T. Stöferle, H. Moritz, C. Schori, M. Köhl, and T. Esslinger, Phys. Rev. Lett. **92**, 130403 (2004).
[31] M. Greiner, I. Bloch, O. Mandel, T. W. Hänsch, and T. Esslinger, Phys. Rev. Lett. **87**, 160405 (2001).
[32] C. A. Regal and D. S. Jin, Phys. Rev. Lett. **90**, 230404 (2003).
[33] A. Polkovnikov, Ann. Phys. (Amsterdam) **325**, 1790 (2010).
[34] A. P. Itin and P. Törmä, Phys. Rev. A **79**, 055602 (2009).
[35] A. Kantian, A. J. Daley, P. Törmä, and P. Zoller, New J. Phys. **9**, 407 (2007).